Chemosphere 220 (2019) 1075–1082

Contents lists available at ScienceDirect

Chemosphere

journal homepage: www.elsevier.com/locate/chemosphere

Application of a microbial fuel cell-based biosensor for the energy-saving operation of macrophyte residues bioreactor with low concentration of dissolved organic carbon in effluents

Chunliu Wang [a, b], Zongbao Yao [a], Leilei Bai [a, b], Changhui Wang [a], Helong Jiang [a, *]

[a] State Key Laboratory of Lake Science and Environment, Nanjing Institute of Geography and Limnology, Chinese Academy of Sciences, Nanjing, 210008, China
[b] University of Chinese Academy of Sciences, Beijing, 100049, China

HIGHLIGHTS

- Linear relationship between DOC concentration in leachate and MFC voltage existed.
- MFC was integrated with MRBR for monitoring DOC concentrations in effluent.
- Aeration could reduce DOC concentration in effluent of MRBR effectively.
- Energy consumption of MRBR would be reduced according to MFC voltage signal.

ARTICLE INFO

Article history:
Received 23 April 2018
Received in revised form
26 November 2018
Accepted 31 December 2018
Available online 2 January 2019

Handling Editor: Chang-Ping Yu

Keywords:
Microbial fuel cell
Dissolved organic carbon
Macrophyte residues bioreactor
Aeration rate
Energy-saving

ABSTRACT

The increasing application of plant residues bioreactor for aquatic environment remediation may release numerous dissolved organic carbon (DOC) into aquatic ecosystems. In this study, a microbial fuel cell (MFC) sensor was integrated with a macrophyte residues bioreactor (MRBR) to provide an energy-saving way for reduction of DOC concentrations in the effluent. Through re-utilization of macrophyte residues as solid carbon source, DOC concentrations in the effluent of MRBR increased to the maximum on day 5 and then dropped down rapidly to a low value, while the ratio of bioavailable DOC decreased gradually. Interestingly, it was found that there existed a linear relationship between DOC concentrations in initial residue leachate and the voltage from MFC biosensor ($R^2 = 0.9852$). Accordingly, aerobic biofilm through aeration were applied in the upper part of MRBR to enhance the degradation of DOC prior to discharge to aquatic systems, and aeration rate was adjusted based on MFC sensor signal. Further experiments demonstrated that when voltage decreased from 0.18 V to 0.09 V, a half of aeration rate (7.5 L min^{-1}) could still lead to a high DOC degradation efficiency (above 50%) and a low DOC concentration (~10 mg L^{-1}) in the reactor effluent. Thus, the integrated MFC signal could be used to regulate the aeration rate in order to obtain a low DOC concentration in effluents under an energy-saving way.

1. Introduction

Plant-based bioreactor, which used plant residues or wood chips as carbon sources, is widely applied to reduce the contaminant loadings to surface waters from agricultural subsurface drainage and groundwater due to its convenience, easy operation, and low cost (Halaburka et al., 2017; Satake and Tang, 2018.; Hua et al., 2016). However, the application of plant-based bioreactor may lead to a number of potential adverse environmental impacts, such as production of greenhouse gases (e.g., N_2O), formation of methyl mercury, and release of dissolved organic carbon (DOC) (Schipper et al., 2010; Shih et al., 2011; Warneke et al., 2011). Among them, DOC is of vital importance to the dynamics of stream and river ecosystems (Stanley et al., 2012), and serves as an index of quality to reflect the organic matter pollution in aquatic environment (Nguyen and Hur, 2011; Spencer et al., 2012). High-concentration leachates from plant residues may pose risks to the aquatic life due to the depletion of oxygen in waters caused by DOC

* Corresponding author. Nanjing Institute of Geography and Limnology, Chinese Academy of Sciences, 73 East Beijing Road, Nanjing, 210008, PR China.
E-mail address: hljiang@niglas.ac.cn (H. Jiang).

https://doi.org/10.1016/j.chemosphere.2018.12.209
0045-6535/

biodegradation. The biodegradation of DOC also influences the optic properties of receiving water (Zhang et al., 2009). Therefore, reducing DOC concentrations in effluent is necessary against the adverse effect of plant-based bioreactor on aquatic systems especially surface water environments.

Microbial fuel cell (MFC) is a device that produce electricity from the oxidation of organic or inorganic fuel by microorganisms (Lovley, 2012; Logan and Rabaey, 2012; Wang et al., 2011). Specifically, microorganisms in the anode compartment can act as biological recognition element whereas electrodes and proton exchange membrane (optional) serve as a transducer (Kumlanghan et al., 2007), offering a great potential of MFCs to be used as a biosensor (ElMekawy et al., 2018). The application of MFC as biosensors has the three following advantages: (i) MFC is established as a real-time shock sensor due to the fact that fuel change causes the immediate jump or drop of voltage signals from MFC; (ii) MFC is self-sustainable and no external power supply is required; (iii) the absence of coating external enzymes and bacteria simplifies the establishment and prolongs the lifetime of MFC (Xu et al., 2015; El Mekawy et al., 2019). Therefore, MFC can be used as an effective online monitoring of organic pollutants and characteristics in environment system through determining the changes in voltage signals. Up to now, many sensors, including biological oxygen demand (BOD) sensor (Modin and Wilén, 2012; Chee et al., 1999), chemical

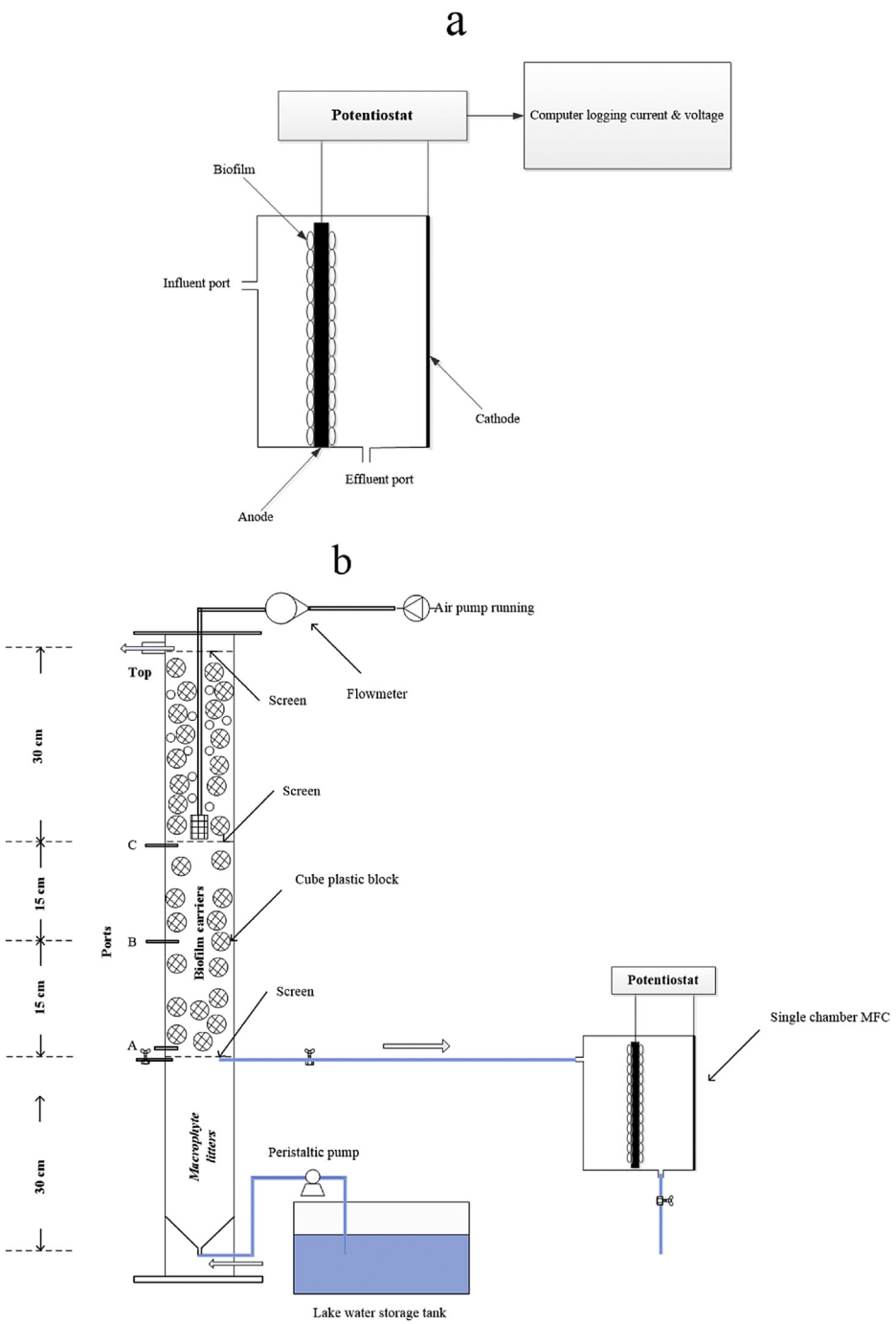

Fig. 1. The structure of single chamber MFC (a) and the schematic diagram of the SMRBR installed with MFC sensor (b).

oxygen demand (COD) sensor (Wang et al., 2014; Xu et al., 2017), dissolved oxygen sensor (Zhang and Angelidaki, 2012), and toxins sensor (Jiang et al., 2015, 2017), have been developed on the basis of MFC technology to monitor aquatic environments.

Additionally, MFC has been applied with bioreactor operations in recent years for monitoring operation state and improving pollutant removal. According to voltage signals, the integration of MFC has successfully reflect the running status of a variety of reactors, such as up-flow anaerobic sludge blanket and up-flow anaerobic fixed biofilm reactor (Yang et al., 2018.; Jia et al., 2017.; Zhang et al., 2012.). However, the feasibility of MFC as a sensor to monitor and then regulate DOC concentrations in the effluent in plants residues bioreactors is still unknown.

The aim of the current study is to develop a MFC-based sensor for detection of DOC concentrations in leachate to obtain low concentrations of DOC in effluent from macrophyte residues bioreactor (MRBR). Relationships between concentrations of DOC in leachate from macrophyte residues and voltage signals produced from MFC was established, and then the DOC degradation was regulated through adjusting aeration rate according to voltage signal from MFC sensor for the energy-saving. This study would help optimize the bioreactor operation with energy saving against adverse effects.

2. Materials and methods

2.1. Sediment and macrophyte residues leachate sampling and preparation

Samples of surface sediment were taken using a Pedersen grab sampler from the Xuanwu Lake (32.07 N, 118.79 E), a eutrophic shallow freshwater lake in Nanjing City, China. After transported to the laboratory within 1 h, the plant debris and macrofauna in sediments were removed by sieving through a 2-mm sieve. Then the sediments were homogenized prior to bioanodes enrichment.

Macrophytes collected from the Xuanwu Lake were air-dried for 48 h and sterilized by 75% ethanol. Then the leachates on days 5 (Le-5) and 20 (Le-20) were collected and diluted with filtered lake water (0.45 μm, Whatman GF/F), respectively. All leachates were sparged with nitrogen gas for 15 min to remove oxygen before adding into MFC.

2.2. MFC construction

A single-chamber MFC was constructed using a cylindrical plexiglas chamber with an inner volume of 100 mL (Fig. 1a). All anodes (3 cm inner diameter) were made of graphite felt with a thickness of 5 mm. The anodes were soaked in 1 M HCl for 24 h and washed with deionized water three times before use. The electrodes were connected to an external circuit using copper wires. The joints were sealed with conductive silver epoxy glue and insulating epoxy glue in succession. The cathode (3 cm inner diameter) was prepared according a procedure described in the Supporting Information. (Cheng et al., 2006). The length of electrode space was 2.5 cm (between the center of anode and the surface of cathode). The circuit was connected through a resistance of 1000 Ω for MFC.

2.3. Inoculum, and enrichment of bioanode

The bioanodes were incubated in the sediment MFCs at 25 °C and a stable voltage signal was measured after 2 months. Then the bioanodes act as anodes of the single chamber MFC with nutrient solutions containing (per L lake water) 6 g Na_2HPO_4, 3 g KH_2PO_4, 0.5 g NaCl, 0.1 g $MgSO_4 \cdot 7H_2O$, 0.015 g $CaCl_2$, and 1 mL trace

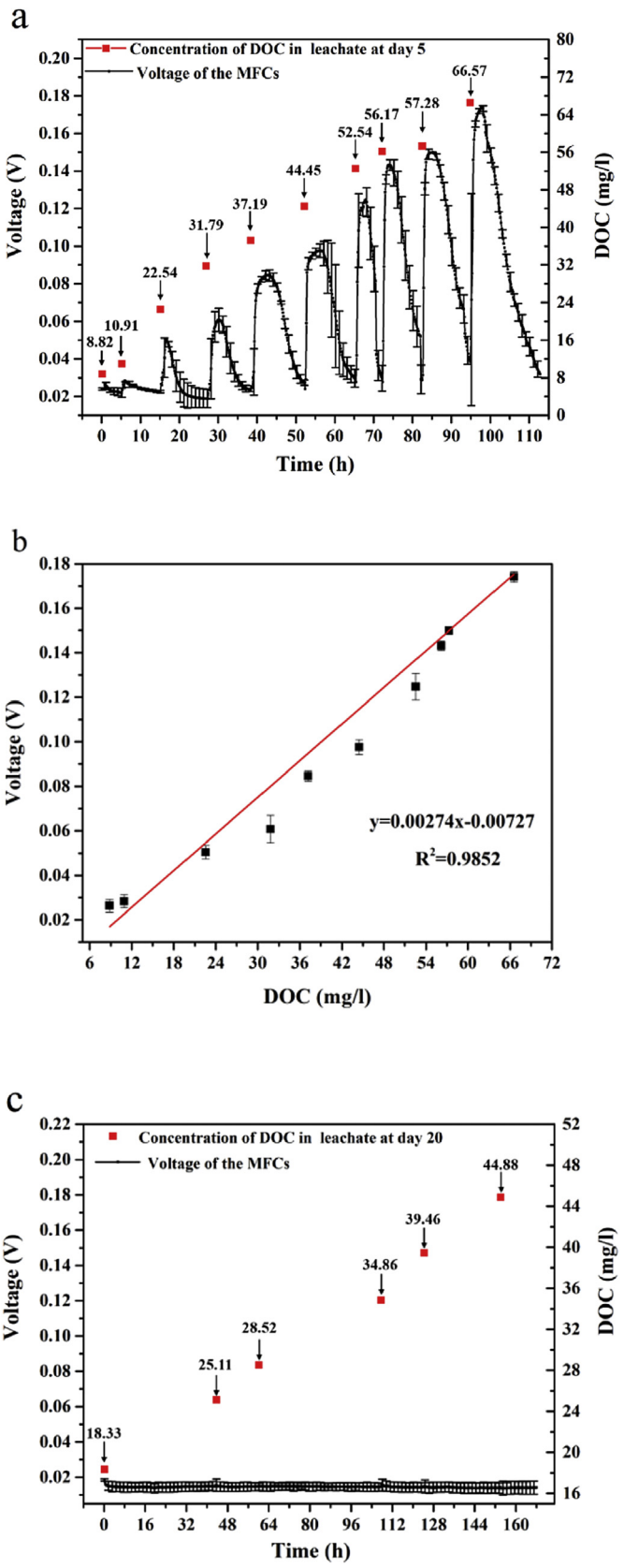

Fig. 2. Changes in voltages from MFCs with different concentrations of Le-5 (a), and the relationship between voltage signals of the MFC sensors and the DOC concentrations (8.82–66.56 mg L-1) of Le-5 (b). Changes in voltages of MFC with different concentrations (from 18.33 to 44.88 mg L-1) of Le-20 (c).

nutrients solution (Lu et al., 2006). The Le-5 was supplied into the MFC as a carbon source for microbial growth for 1 month, with a stable voltage output of ~20 mV. All MFC experiments were conducted in duplicate.

2.4. The bioavailability of DOC released from macrophyte residues

A 4-stage plug-flow bioreactor was applied to determine the bioavailability of DOC in leachates from macrophyte residues, as described previously (Bai et al., 2017). The bioreactor consisted of 4 tandem darkened glass reactors with different volumes. The stored Le-5 and Le-20 were pumped as influents and samples were collected from effluent of each reactor (Eff-1, Eff-2, Eff-3, and Eff-4, respectively) for DOC analysis. The labile, semilabile and refractory fractions of DOC were calculated by *G* model:

$$DOC = C_1 e^{-k1 \cdot t} + C_2 e^{-k2 \cdot t} + C_2 e^{0} \quad (1)$$

where C_1, C_2 and C_3 were the concentrations of labile, semilabile and refractory DOC, respectively.

2.5. MRBR experimental system

In this study, The MRBR was used to remove NO_3^--N (~8 mg L^{-1}) from surface water, and the up-flow column reactors were built with macrophyte residues as carbon substrate (Fig. 1b), and the macrophyte residues were refilled every 90 days. Plastics multi-hole screens were placed to divide the MRBR into 3 segments, each of which was 30 cm high. The bottom of reactor was filled with macrophyte residues to provide carbon source for microbial growth. Meanwhile, MFC sensors were applied to monitor the concentration of DOC in A-port's discharge. The upper 2 segments were filled with cube plastic carriers for microbial development, these carriers were made of polypropylene with a diameter of only 10 mm and could be recycled and reused. Aeration device in the top part of MRBR was controlled by a flowmeter. The lake water (5–8 mg NO_3^--N L^{-1}) was pumped into the bottom of MRBR by a peristaltic pump. The total hydraulic retention time was 6 h.

2.6. Experimental analysis

2.6.1. Electrochemical analysis

The voltage was recorded with a Keithley model 2700 multimeter (Keithley Instruments 2700, USA) every 10 min. The measured voltage was converted to current according to Ohm's law: V=IR, and power according to P=VI, respectively. Electricity current and power density were calculated on the basis of anodic geometric surface areas (GA). For polarizations behavior test of MFC, linear sweep voltammetry (LSV) was employed by recording the current at an applied voltage. The voltage was lowered in steps of 0.001 V from open-circuit voltage to 0 V with electrochemical workstation (CHI660D, Shanghai Chenhua Device company, China), during which anodes were considered as working electrodes and cathodes as counter electrodes. According to the polarization curve, power curves describing the power density as a function of current density were obtained. Internal resistance was calculated by the polarization slope method (Song and Jiang, 2018).

2.6.2. Chemical and spectral analysis

NO_3^- concentrations in water samples were determined by an automated flow injection analyzer (Smartchem 200, AMS Alliance, Rome, Italy) using the online digestion flow injection analysis method. The pH level (pH 10, Sartorius, Germany), dissolved oxygen (DO) (JPB-607 A, REX Instrument Factory, Shanghai, China) were monitored in 20 days. DOC concentrations in water samples

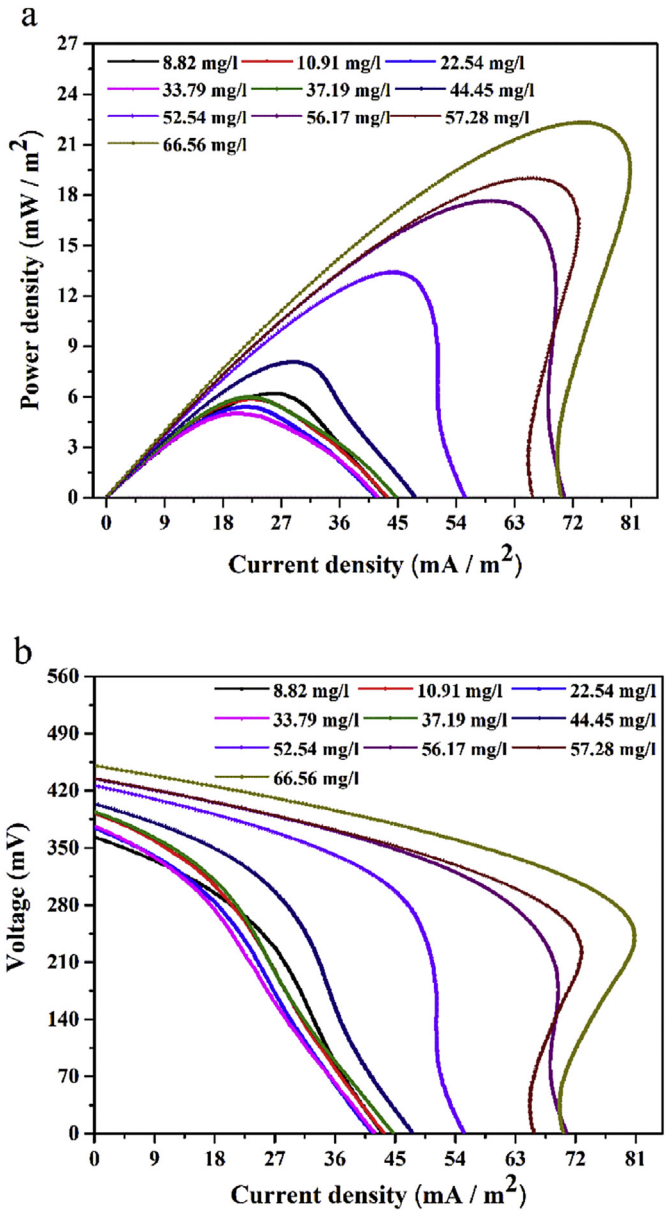

Fig. 3. Electrochemical properties of MFC with different DOC concentrations of Le-5, including power curves (a), polarization curves (b).

Table 1
The bioavailability of DOC in A-port's effluent at day 5 and 20.

Day	Bioavailability of DOC in effluent at day 5			Bioavailability of DOC in effluent at day 20		
Types of DOC	Labile DOC	Semi-labile DOC	Refractory DOC	Labile DOC	Semi-labile DOC	Refractory DOC
Concentrations (mg L^{-1})	45.1	22.88	27.05	3.48	7.11	20.97
Proportion (%)	47.45	24.07	28.46	11.03	22.53	66.44

were determined as non-purgeable organic carbon using a total organic carbon analyzer (Torch, Teledyne Tekmar, USA). The UV–Vis absorption spectra of samples were measured by a Shimadzu 2000 spectrometer (Shimadzu Corp, Japan). The fluorescence spectrums of samples were measured using an F-7000 fluorescence spectrometer (Hitachi High Technologies, Japan). The absorbance and fluorescent DOC characteristic parameters, including a_{254}, specific UV absorbance ($SUVA_{254}$) were determined with detailed methods described elsewhere (Bittar et al., 2015). Fluorescent dissolved organic matter (FDOM) components were identified by the parallel factor analysis (PARAFAC) modeling using drEEMs toolbox (ver. 0.2.0) for MATLAB (R2012a) (Murphy et al., 2013).

2.6.3. Statistical analysis

The means and standard deviations were calculated using Origin 8.5. Statistical significance of correlation was determined by one - way analysis of variance using the SPSS software (IBM SPSS Statistics 19). The correlations were considered statistically significant at a 95% confidence internal with $p < 0.05$.

3. Results and discussion

3.1. The composition and bioavailability changes of DOC leached from macrophyte residues at different stages

According to previous studies, MFC could consume proteins (Heilmann and Logan, 2006), carbohydrates (Niessen et al., 2004), and small organic molecules (Liu et al., 2005; Min et al., 2005) to produce electricity at a high efficiency. The four-component PARAFAC model was well validated to identify the number of components in leachate from macrophyte residues. The spectral characteristics of the four components (Fig. 2a and b) were similar to the previously identified components in aquatic environments (Kim et al., 2006). The spectra of component 1 (C1) consisted of two excitation peaks at Ex220, 275/Em337 nm and was ascribed to aromatic protein-like substances. Component 2 (C2) exhibited an excitation and emission spectrum with maxima at Ex 235, 305/Em427 nm, similar to a fulvic acid-like substance. For component 3 (C3), a duo peak at Ex/Em < 275/471 and 365/471 nm can be denoted as a humic acid-like substance. Component 4 (C4) (Ex 255, 290/Em343 nm) was categorized as a traditional tryptophan-like component. As shown in Fig. 2c, the fluorescence intensity for FDOM increased to the maximum on day 5, and then decreased to a stable stage. The fluorescence intensity of C1 and C4 displayed a strong linear correlation with the fluorescence intensity of FDOM ($P < 0.05$, $r > 0.9$, $N = 18$), suggesting that the protein-like substances may be a proxy for labile DOM components. The significant role of C1 and C4 in DOM biodegradation was also previously reported (Fellman et al., 2008; Hosen et al., 2014). Moreover, the value of $SUVA_{254}$ dropped to the minimum during the initial 5 days, then gradually increased (Fig. 2d). The increase in $SUVA_{254}$ suggested that the dominant component of light-absorbing DOC transformed to humic-like substances with a higher aromaticity (He et al., 2016).

The proportions of the labile, semilabile and refractory fractions in Le-5 and Le-20 were quantified by *G* model fitting (Fig. S1). The labile and semilabile fractions of DOC were easily consumed and decomposed by microbes (Hanamachi et al., 2008), while the

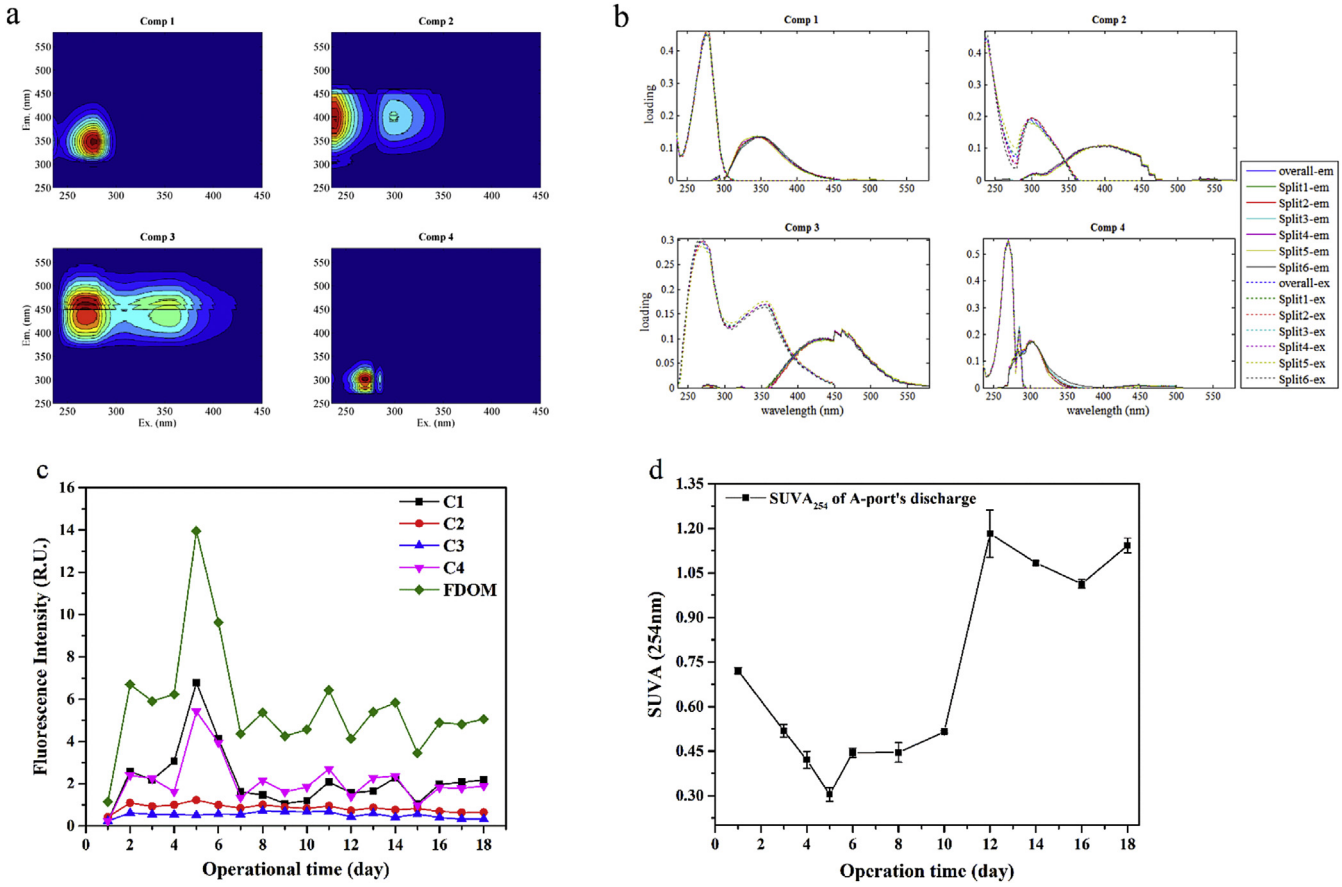

Fig. 4. EEM spectrum of the 4 components identified by the PARAFAC analysis for the DOM samples (a) and the highly overlaid excitation and emission spectra estimated using the split-half validation procedure. (b), The fluorescence intensity (R.U.) changes of 4 different components during 20 days (c) and the variation of SUVA254 in 20 days (d).

refractor fraction was decomposed slowly and remained almost constant. The labile and semilabile fractions (C1, C4) in the Le-5 sample were the major components of DOC (>50%), while more than 66% was composed of recalcitrant fractions (C2, C3) in the Le-20 sample (Table 1).

3.2. Effect of DOC concentrations of leachate from macrophyte residues on MFC voltage

With the increasing interests in the nitrate removal, many advanced biotechnologies were proposed. For example, the bioelectrochemical treatment of complex wastewaters containing nitrate has been shown to be an effective remediation approach at lab scale, however, the low conductivity of surface water (<1.5 mS/cm) should be taken into account for the system efficiency (Sevda et al., 2018). In this study, the MRBR was operated to reduce nitrate in the surface water, and the nitrate concentrations of effluents for 4 different ports of MRBR were shown in Table S1. It showed that the nitrate in the C-port's discharge was almost removed with aeration during 60 days operation. In the MRBR, the short-term release of DOC during the reactor startup was characterized by an initial high release followed by a rapid decline (Schipper et al., 2010). To get relationships between DOC concentrations and voltage signals, a series of leachate samples with different concentrations of Le-5 and Le-20 were obtained for MFC testing experiments. The addition of various concentrations of Le-5 led to a change of voltage signals in MFCs (Fig. 3a). It was obvious that the voltage signals increased to a maximum value (from 26.36 to 174.16 mV) about 3 h later after the supply of leachates with DOC concentrations from 8.82 to 66.56 mg L^{-1}. The relationship between DOC concentrations and maximum voltage signals was described well by the first order kinetic model. As shown in Fig. 3b, the maximum voltage signals increased linearly ($R^2 = 0.9852$) with DOC concentrations. This suggested that DOC concentrations could be calculated by the voltage at the rapid release phase. However, voltage signals for Le-20 were almost kept at a stable value, even the concentrations of DOC changed from 18.33 mg L^{-1} to 44.88 mg L^{-1} (Fig. 3c). The different relationships between DOC concentrations and voltage signals for Le-5 and Le-20 can be attributed to the differences in the composition and bioavailability of DOC. The composition of DOC changed from labile to refractory fractions gradually, and voltage signals from MFC decreased to a stable value in 20 days. The concentration changes in C1 and C4 fractions affected the microbial activity on the anodes, so the voltage signals of MFCs were also changed.

3.3. Electrochemical properties of MFC sensors

The LSV responded to the change in DOC concentrations of leachates after the addition of different concentrations of Le-5 into the MFC. According to the polarization curve (Fig. 4a), the power density increased with the concentration of DOC, the maximum power density increased slowly for DOC concentrations less than 37.19 mg L^{-1}. However, the maximum power density increased dramatically, when the concentrations of DOC ranged from 44.45 mg L^{-1} to 66.56 mg L^{-1}. The maximum power density reached to 22.32 mW m^{-2} at a DOC concentration of 66.56 mg L^{-1}. A unique feature, power overshoot (Fig. 4a and b), was attributed to the decreasing internal resistance (Hong et al., 2011). As shown in Fig. 4b, the slope of curves increased gradually and the internal resistance of the MFC dropped simultaneously. The internal resistance decreased from 3354.45 Ω to 849.70 Ω with DOC concentrations changing from 8.82 mg L^{-1} to 66.56 mg L^{-1}. The results were almost same as MFC with conventional substrates such as acetate or real wastewaters (Pasupuleti et al., 2016; Pant et al., 2016). High power density and voltage signals were obtained at high DOC concentrations, suggesting that more DOC was consumed for power generation (Xu et al., 2017). Specifically, the rate of the maximal power density gradually reduced as the utilization of DOC saturated gradually (Xu et al., 2017; Logan, 2008).

3.4. The integration of MFC sensors with MRBR

During a 20-day operation of MRBR, the concentration of DOC in the discharge of A-port had a high variation. Because of abundant DOC removal, the generation of H^+ ions might lead to decrease in pH and DO level. In this study, it was found that the pH and DO of effluent decreased on day 5 (Fig. S2), but the reduced values were low. As shown in Fig. 5a, DOC concentration in effluent decreased from 98.16 mg L^{-1} to 18.82 mg L^{-1} after 12 days of operation at an HRT of 6 h. The DOC leached during this period could represent readily soluble organic compounds from plant residues, and the release rates of the pre-existing DOC were likely controlled by the mass transfer across the liquid film surrounding the plant residues (Abusallout and Hua, 2017). Meanwhile, the concentration of DOC

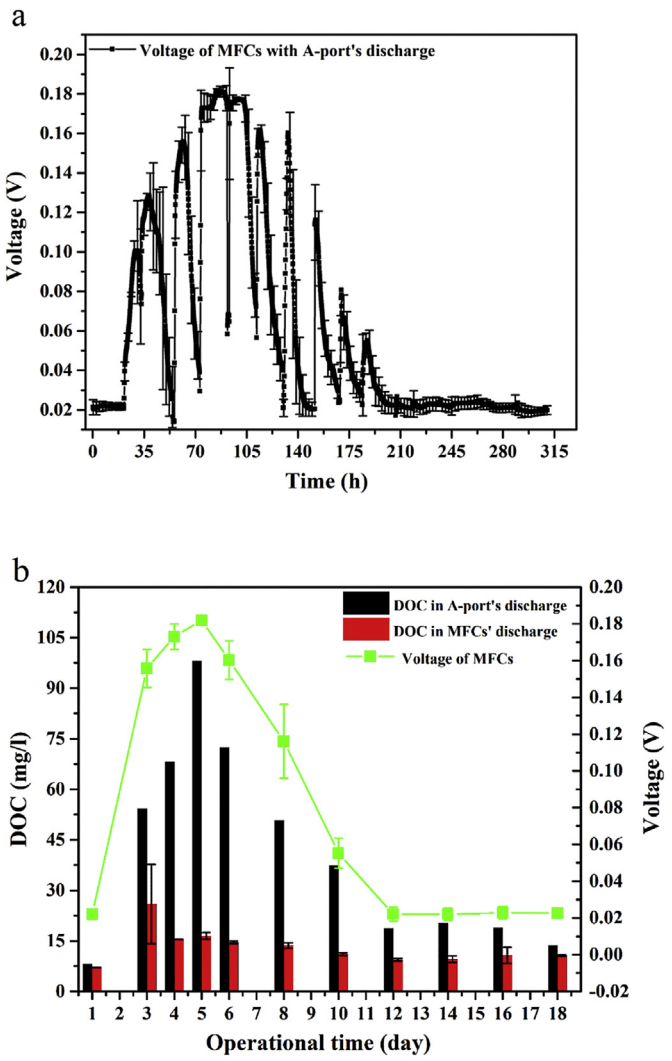

Fig. 5. The variation of voltage signals with discharge from A-port of SMRBR during 20 days' operation time (a). The concentrations of DOC in discharge from A-port (black bar) and the discharge of the MFCs (red bar), combined with the voltage changes during 20 days' operation (b). (For interpretation of the references to colour in this figure legend, the reader is referred to the Web version of this article.)

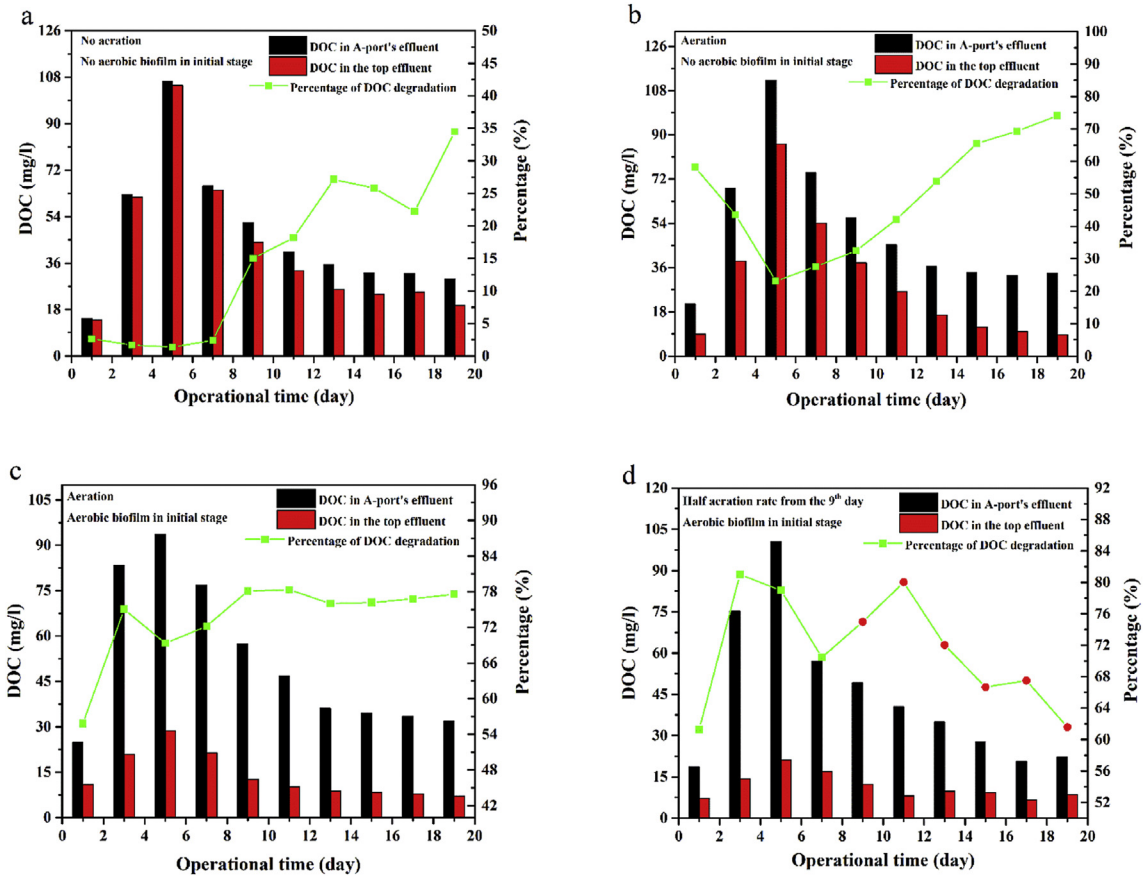

Fig. 6. The concentrations of DOC in the A-port's discharge and effluent changed along with aeration and biofilm during 20 days, the percentage of the DOC degradation in 4 different conditions which the concentrations of DOC changed with no aeration and no aerobic biofilm in initial stage (a), aeration and no aerobic biofilm in initial stage (b), aeration and aerobic biofilm in initial stage (c), half aeration rate on the day 9 (d).

in A-port had a similar variation trend with voltage signals from MFC, and the value of voltage signal reached to the highest level (0.18 V) on day 5 and subsequently deceased approximately to 0.022 V (Fig. 5b). These results suggested that the variation of DOC concentrations corresponded to the values of voltage signals. In addition, concentrations of DOC in MFC decreased to around 15 mg L^{-1} (Fig. 5b) as most of the labile fractions in DOC was converted to electrical energy by bioanodes (Wang et al., 2017).

3.5. The reduction of DOC concentration in effluent based on MFC signal

Compared with anaerobic biofilm, labile DOC can be rapidly utilized by aerobic biofilm (McKew et al., 2013). So, the three MRBRs with and without aeration and biofilms were established to investigate the removal efficiency of DOC in the reactors. As shown in Fig. 6, aeration and biofilm had obvious effects on DOC concentrations in effluents. Without aerobic biofilm and aeration in the top part of MRBR in the initial stage, DOC removal in effluents was low (less than 10%) in the initial 5 days (Fig. 6a). Although a higher removal efficiency (above 30%) was achieved with aeration, DOC concentration (around 86.20 mg L^{-1}) in effluent were still high (Fig. 6b). However, the combination of aerobic aeration and biofilm in the top part of MRBR lead to the highest degradation efficiency (above 70%) and the lowest concentration of DOC (28.74 mg L^{-1}) in effluents, even the concentration of DOC in A-port's discharge was 93.63 mg L^{-1} on day 5 (Fig. 6c).

To reduce the energy consumption from aeration, the aeration rate was then regulated according to voltage signals of MFC. When the voltage signals fell to half of the maximum (0.09 V) on day 9, the aeration rate was reduced from 15 to 7.5 L min^{-1}. As shown in Fig. 6d, DOC concentrations in effluents of MRBR still decreased around 10 mg L^{-1} (red bar) with a high degradation efficiency (above 50%) (red point). These outcomes indicated that a decrease in aeration rate according to the voltage signals of MFC can keep the low concentration of DOC in effluent.

4. Conclusions

To achieve a low DOC concentration and high degradation efficiency for effluent in the MRBR, aeration rate and aerobic biofilm were used in the top part of MRBR. Then the study showed that the MFC sensor, integrated with the MRBR, could be used to regulate the aeration rate in order to obtain a low DOC concentration in effluents under an energy-saving way. The linear relationship ($R^2 = 0.9852$) between concentration of DOC in leachate and voltage from MFC was established to monitor DOC concentrations in effluent of MRBR. Based on the relationship, reducing aeration rate by half when voltage produced from MFC decreased from 0.18 V to 0.09 V still can keep a low DOC concentration (~10 mg L^{-1}) and a high DOC degradation efficiency (above 50%) in effluent. As a result, the research provides a valuable guide for the future development of the plant-based bioreactor.

Acknowledgements

This work was supported by grants from National Natural Science Foundation of China (51839011, and 51679228, 51861125201),

CAS Interdisciplinary Innovation Team, and the Major Science and Technology Program for Water Pollution Control and Treatment (2017ZX07204005) .

Appendix A. Supplementary data

Supplementary data to this article can be found online at https://doi.org/10.1016/j.chemosphere.2018.12.209.

References

Abusallout, I., Hua, G., 2017. Characterization of dissolved organic carbon leached from a woodchip bioreactor. Chemosphere 183, 36–43.

Bai, L., Cao, C., Wang, C., Xu, H., Zhang, H., Slaveykova, V.I., et al., 2017. Toward quantitative understanding of the bioavailability of dissolved organic matter in freshwater lake during cyanobacteria blooming. Environ. Sci. Technol. 51, 6018.

Bittar, T.B., Vieira, A.A.H., Stubbins, A., et al., 2015. Competition between photochemical and biological degradation of dissolved organic matter from the cyanobacteria Microcystis aeruginosa. Limnol. Oceanogr. 60, 1172–1194.

Chee, G.J., Nomura, Y., Karube, I., 1999. Biosensor for the estimation of low biochemical oxygen demand. Anal. Chim. Acta 379, 185–191.

Cheng, S., Liu, H., Logan, B.E., 2006. Power densities using different cathode catalysts (Pt and CoTMPP) and polymer binders (Nafion and PTFE) in single chamber microbial fuel cells. Environ. Sci. Technol. 40, 364–369.

ElMekawy, A., Hegab, H.M., Pant, D., et al., 2018. Bio-analytical applications of microbial fuel cell–based biosensors for onsite water quality monitoring. J. Appl. Microbiol. 124, 302–313.

El Mekawy, A., Hegab, H.M., Mohanakrishna, G., et al., 2019. Integrated Bioelectrochemical Platforms[M]//Microbial Electrochemical Technology. Elsevier, pp. 1037–1058.

Fellman, J.B., D'Amore, D.V., Hood, E., Boone, R.D., 2008. Fluorescence characteristics and biodegradability of dissolved organic matter in forest and wetland soils from coastal temperate watersheds in southeast Alaska. Biogeochemistry 88, 169–184.

Halaburka, B.J., LeFevre, G.H., Luthy, R.G., 2017. Evaluation of mechanistic models for nitrate removal in woodchip bioreactors. Environ. Sci. Technol. 51, 5156–5164.

Hanamachi, Y., Hama, T., Yanai, T., 2008. Decomposition process of organic matter derived from freshwater phytoplankton. Limnology 9, 57–69.

He, W., Chen, M., Park, J.E., et al., 2016. Molecular diversity of riverine alkaline-extractable sediment organic matter and its linkages with spectral indicators and molecular size distributions. Water Res. 100, 222–231.

Heilmann, J., Logan, B.E., 2006. Production of electricity from proteins using a microbial fuel cell. Water Environ. Res. 78, 531–537.

Hosen, J.D., McDonough, O.T., Febria, C.M., Palmer, M.A., 2014. Dissolved organic matter quality and bioavailability changes across an urbanization gradient in headwater streams. Environ. Sci. Technol. 48, 7817–7824.

Hong, Y., Call, D.F., Werner, C.M., Logan, B.E., 2011. Adaptation to high current using low external resistances eliminates power overshoot in microbial fuel cells. Biosens. Bioelectron. 28, 71–76.

Hua, G., Salo, M.W., Schmit, C.G., Hay, C.H., 2016. Nitrate and phosphate removal from agricultural subsurface drainage using laboratory woodchip bioreactors and recycled steel byproduct filters. Water Res. 102, 180–189.

Jiang, Y., Liang, P., Zhang, C., et al., 2015. Enhancing the response of microbial fuel cell- based toxicity sensors to Cu(II) with the applying of flow-through electrodes and controlled anode potentials. Bioresour. Technol. 190, 367.

Jiang, Y., Liang, P., Liu, P., et al., 2017. A novel microbial fuel cell sensor with biocathode sensing element. Biosens. Bioelectron. 94, 344–350.

Jia, H., Yang, G., Ngo, H.H., Guo, W., Zhang, H., Gao, F., Wang, J., 2017. Enhancing simultaneous response and amplification of biosensor in microbial fuel cell-based upflow anaerobic sludge bed reactor supplemented with zero-valent iron. Chem. Eng. J. 327, 1117–1127.

Kim, S., Kaplan, L.A., Hatcher, P.G., 2006. Biodegradable dissolved organic matter in a temperate and a tropical stream determined from ultra - high resolution mass spectrometry. Limnol. Oceanogr. 51, 1054–1063.

Kumlanghan, A., Liu, J., Thavarungkul, P., et al., 2007. Microbial fuel cell-based biosensor for fast analysis of biodegradable organic matter. Biosens. Bioelectron. 22, 2939–2944.

Liu, H., Cheng, S., Logan, B.E., 2005. Production of electricity from acetate or butyrate using a single-chamber microbial fuel cell. Environ. Sci. Technol. 39, 658–662.

Lu, H., Oehmen, A., Virdis, B., et al., 2006. Obtaining highly enriched cultures of Candidatus Accumulibacter phosphates through alternating carbon sources. Water Res. 40, 3838–3848.

Lovley, D.R., 2012. Electromicrobiol. Annual Rev. Microbiol. 66, 391–409.

Logan, B.E., Rabaey, K., 2012. Conversion of wastes into bioelectricity and chemicals by using microbial electrochemical technologies. Science 337, 686–690.

Logan, B.E., 2008. Microbial Fuel Cells. John Wiley & Sons.

McKew, B.A., Dumbrell, A.J., Taylor, J.D., McGenity, T.J., Underwood, G.J., 2013. Differences between aerobic and anaerobic degradation of icrophytobenthic biofilm-derived organic matter within intertidal sediments. FEMS Microbiol. Ecol. 84, 495–509.

Min, B., Kim, J., Oh, S., Regan, J.M., Logan, B.E., 2005. Electricity generation from swine wastewater using microbial fuel cells. Water Res. 39, 4961–4968.

Modin, O., Wilén, B.M., 2012. A novel bioelectrochemical BOD sensor operating with voltage input. Water Res. 46, 6113–6120.

Murphy, K.R., Stedmon, C.A., Graeber, D., et al., 2013. Fluorescence spectroscopy and multi-way techniques. PARAFAC. Analytical Method. 5, 6557–6566.

Niessen, J., Schröder, U., Scholz, F., 2004. Exploiting complex carbohydrates for microbial electricity generation — a bacterial fuel cell operating on starch. Electrochem. Commun. 6, 955–958.

Nguyen, H.V.M., Hur, J., 2011. Tracing the sources of refractory dissolved organic matter in a large artificial lake using multiple analytical tools. Chemosphere 85, 782–789.

Pant, D., Van Bogaert, G., Alvarez-Gallego, Y., et al., 2016. Evaluation of bioelectrogenic potential of four industrial effluents as substrate for low cost Microbial Fuel Cells operation. Environ. Eng. Manag. J. (EEMJ) 51, 8.

Pasupuleti, S.B., Srikanth, S., Dominguez-Benetton, X., et al., 2016. Dual gas diffusion cathode design for microbial fuel cell (MFC): optimizing the suitable mode of operation in terms of bioelectrochemical and bioelectro-kinetic evaluation. J. Chem. Technol. Biotechnol. 91, 624–639.

Satake, S., Tang, C., 2018. Groundwater nitrate remediation using plant-chip bioreactors under phosphorus-limited environment. J. Contam. Hydrol. 209, 42–50.

Sevda, S., Sreekishnan, T.R., Pous, N., et al., 2018. Bioelectroremediation of perchlorate and nitrate contaminated water: a review. Bioresour. Technol. 255, 331–339.

Song, N., Jiang, H.L., 2018. Effects of initial sediment properties on start-up times for sediment microbial fuel cells. Int. J. Hydrogen Energy 43, 10082–10093.

Shih, R., Robertson, W.D., Schiff, S.L., Rudolph, D.L., 2011. Nitrate controls methyl mercury production in a streambed bioreactor. J. Environ. Qual. 40, 1586–1592.

Spencer, R.G.M., Butler, K.D., Aiken, G.R., 2012. Dissolved organic carbon and chromophoric dissolved organic matter properties of rivers in the USA. J. Geophys. Res.: Biogeosci. 117 (G3).

Stanley, E.H., Powers, S.M., Lottig, N.R., et al., 2012. Contemporary changes in dissolved organic carbon (DOC) in human-dominated rivers: is there a role for DOC management? Freshw. Biol. 57, 26–42.

Schipper, L.A., Robertson, W.D., Gold, A.J., Jaynes, D.B., Cameron, S.C., 2010. Denitrifying bioreactors-An approach for reducing nitrate loads to receiving waters. Ecol. Eng. 36, 1532–1543.

Wang, J., Zheng, Y., Jia, H., et al., 2014. Bioelectricity generation in an integrated system combining microbial fuel cell and tubular membrane reactor: effects of operation parameters performing a microbial fuel cell-based biosensor for tubular membrane bioreactor. Bioresour. Technol. 170, 483–490.

Wang, A., Sun, D., Cao, G., et al., 2011. Integrated hydrogen production process from cellulose by combining dark fermentation, microbial fuel cells, and a microbial electrolysis cell. Bioresour. Technol. 102, 4137–4143.

Wang, Y., Feng, C., Li, Y., Gao, J., Yu, C.P., 2017. Enhancement of emerging contaminants removal using Fenton reaction driven by H_2O_2 - producing microbial fuel cells. Chem. Eng. J. 307, 679–686.

Warneke, S., Schipper, L.A., Bruesewitz, D.A., Mcdonald, I., Cameron, S., 2011. Rates, controls and potential adverse effects of nitrate removal in a denitrification bed. Ecol. Eng. 37, 511–522.

Xu, L., Zhao, Y., Fan, C., et al., 2017. First study to explore the feasibility of applying microbial fuel cells into constructed wetlands for COD monitoring. Bioresour. Technol. 243, 846–854.

Xu, Z., Liu, B., Dong, Q., et al., 2015. Flat microliter membrane-based microbial fuel cell as “on-line sticker sensor” for self-supported in situ monitoring of wastewater shocks. Bioresour. Technol. 197, 244–251.

Yang, Z., Pei, H., Hou, Q., Jiang, L., Zhang, L., Nie, C., 2018. Algal biofilm-assisted microbial fuel cell to enhance domestic wastewater treatment: nutrient, organics removal and bioenergy production. Chem. Eng. J. 332, 277–285.

Zhang, B., Zhang, J., Yang, Q., Feng, C., Zhu, Y., Ye, Z., Ni, J., 2012. Investigation and optimization of the novel UASB–MFC integrated system for sulfate removal and bioelectricity generation using the response surface methodology (RSM). Bioresour. Technol. 124, 1–7.

Zhang, Y., Angelidaki, I., 2012. A simple and rapid method for monitoring dissolved oxygen in water with a submersible microbial fuel cell (SBMFC). Biosens. Bioelectron. 38, 189–194.

Zhang, Y., van Dijk, M.A., Liu, M., Zhu, G., Qin, B., 2009. The contribution of phytoplankton degradation to chromophoric dissolved organic matter (CDOM) in eutrophic shallow lakes: field and experimental evidence. Water Res. 43, 4685–4697.